POLITECNICO DI TORINO
Repository ISTITUZIONALE

Digital image correlation applied to lime-based mortars: Shrinkage tests for durability evaluations in restoration works.

*Original*
Digital image correlation applied to lime-based mortars: Shrinkage tests for durability evaluations in restoration works / Grazzini, A., Lacidogna, G., Zerbinatti, M., Fasana, S., Vecchio, F.. - In: DEVELOPMENTS IN THE BUILT ENVIRONMENT. - ISSN 2666-1659. - ELETTRONICO. - 10:(2022), pp. 1-11. [10.1016/j.dibe.2022.100070]

*Availability:*
This version is available at: 11583/2958230 since: 2022-03-22T08:54:39Z

*Publisher:*
Elsevier

*Published*
DOI:10.1016/j.dibe.2022.100070

*Terms of use:*

This article is made available under terms and conditions as specified in the corresponding bibliographic description in the repository

*Publisher copyright*

(Article begins on next page)

27 November 2026

Developments in the Built Environment 10 (2022) 100070

Contents lists available at ScienceDirect

Developments in the Built Environment

journal homepage: www.sciencedirect.com/journal/developments-in-the-built-environment

# Digital image correlation applied to lime-based mortars: Shrinkage tests for durability evaluations in restoration works

Alessandro Grazzini [a,*], Giuseppe Lacidogna [a], Marco Zerbinatti [a], Sara Fasana [a], Federico Vecchio [a]

[a] Politecnico di Torino – Department of Structural Geotechnical Building Engineering, Turin, Italy

ARTICLE INFO

*Keywords:*
Shrinkage
DIC
Repair lime-based mortars
Restoration works
Durability
Laboratory tests

ABSTRACT

Repair mortars applied to architectural heritage buildings for preservation, maintenance, restoration, and strengthening must be carefully studied regarding the many different compatibility issues. In the case of repair interventions, two closely related aspects are especially important: the mortar composition, and the method of its application, which can strongly influence the shrinkage phenomena during the setting and hardening phases. The aim of present experimental research is to set-up a procedure by Digital Imaging Correlation (DIC) technique to deepen shrinkage phenomena in lime-based mortars, thus comparing many different materials, wrongly considered to be similar in behaviour. The technique enable not only shrinkage measurement accuracy higher than standard tests, but also to understand its mechanisms of evolution over time, by evaluating locally strain stress before micro-crack appearing. The interpretation of a large number of test results represents a significant contribution to the development of operational tools to address material selection in specific contexts.

## 1. Introduction

The compatibility relevance of repair mortars in interventions on historic plasters and on mortar layers and joints is well known. Compatibility must be considered as a complex of needs, not only in chemical-physical-mechanical terms, but also in economic, environmental, historical-architectural and aesthetic terms, with an increasing component of "abstract" requirements, for which knowledge and interpretation are indispensable to identify adequate answers. No less complex, but more objectively quantifiable, are the "practical" requirements, generally summarised in the definition of mix-design, which together with the above mentioned ones constitute the background necessary to define, in every specific case, the technological and functional requirements of the repair mortar (C 167-M: Charact, 2005). In fact, consequences of the incorrect use of different mortars with related physical-chemical and mechanical characteristics very different from those of the original ones (often not compatible with the support) are well known (Grazzini et al., 2019). The restoration phase therefore requires not only an in-depth preliminary study regarding the characteristics of the original material affected by decay (Lindqvist, 2009), but also the compatibility of the new repair mortar chosen as a solution for restoring the original finishing and functional integrity of the historic plaster (within the respect of conservation principles concerning the authentic *architectonic matter*). Various experimental tests can be performed in the laboratory to verify the mechanical characteristics of the new repair mortars. For instance fatigue tests can qualify their compatibility with original masonry support (Bocca and Grazzini, 2013; Bocca et al., 2011). The mechanical incompatibility between repair mortars and masonry structures causes the detachment of the strengthening material, thus making ineffective the repair work (Grazzini et al., 2020; Tarizzo et al., 2013).

One of the most insidious phenomena for the durability of restoration work is the shrinkage of the new repair mortars. It is known that during the curing phenomena of concrete or mortar, there is a change in volume known as shrinkage. It is a complex time-depending phenomenon, acting regardless of the loads and originates from the movement of water inside the binding paste. Some factors that influence the shrinkage are the water evaporation and the binder hydration. Moreover, the binder-aggregate ratio and the size distribution of aggregates can reduce the opening of cracks. In the initial stage, the material is in the plastic state and water (known as "purge water") builds up progressively on the exposed surface, to then it dry and evaporate over time. In parallel, the gel pore water is absorbed by the binder particles (especially) and aggregate (in relationship with its porosity). This resulted in the

* Corresponding author.
*E-mail address:* alessandro.grazzini@polito.it (A. Grazzini).

https://doi.org/10.1016/j.dibe.2022.100070
Received 18 December 2021; Received in revised form 12 February 2022; Accepted 25 February 2022
Available online 8 March 2022
2666-1659/© 2022 The Authors. Published by Elsevier Ltd. This is an open access article under the CC BY license (http://creativecommons.org/licenses/by/4.0/).

shrinkage strains and volume loss. In summary, there are three types of shrinkage:

- *plastic or short term*: a few hours after casting, caused by the evaporation of water from casting surface towards an environment with Relative Humidity (R.H.) < 95%. Excessive speed induces (modest) tensile stresses in the material causing surface cracks. This phenomenon is accentuated in structures whit high surface/volume ratio.
- *autogenic or chemical*: a few hours after casting, caused by the hydration process of the binder and the consequent formation of capillary pores. The contraction occurs in the largest pores due to the migration of water into the smaller ones. It depends on the binder and it is modest if compared to the other two types.
- *hygrometric or long-term*: in the first months of maturation, caused by the evaporation of the mixing water towards an environment with R. H. <95%. The contraction is here induced by the migration of the water contained in the pores, causing superficial cracks. It depends on the external temperature (and, obviously, on the exposure), the air speed, and the water/binder ratio (an excess of free water causes shrinkage).

If the occurrence of shrinkage is not reduced or inhibited in the mortar, the shrinkage would inevitably cause aesthetic inconsistencies on the repaired plaster and cracks inside the repair mortar. However, shrinkage can be reduced by using particular precautions during the design of the mixes (e.g., paying attention to the mix-design of aggregates and to the ratio binder/aggregates), or during the laying phase of the technical execution and hardening.

In the restoration mortars, the shrinkage may have different manners to revealing in opera, also in relationship with the final application of the fresh mixture. The causes can be originated by incorrect water/binder ratio on construction site, unsuitable application, or by a wrong chose of the mortar type with regard to the final use.

As is well known, a layer of bed mortar has a different thickness respect a render or the final coat; then, there are some factors that is right to take in account like good practices during the works execution, with the aims to reduce the risks of defects on the different layers. Some examples are specified below:

- the relevance in the choose of the reparation/restoration mortar (choose mortars with mechanical and physical-chemical characteristics similar to the original ones), - the adequate laying techniques of the craftsmen, - the care during the setting and hardening time, above all in difficult environmental conditions.

Possible consequences, among others, of non-optimal choices and/or execution defects are cracking of joint mortars or render layers, detachment of render layers from the support, aesthetic inconsistencies on the architectural palimpsest.

For these issues, the aim of present experimental research is the set-up of specific laboratory tests on shrinkage by Digital Imaging Correlation (DIC) technique, to deepen the trend of this phenomenon on different repair mortars usually applied in recovery interventions. Deep knowledge of shrinkage, together with other characteristics (chemical, mechanical, e.g.), will contribute to enabling adequate choices towards higher durability when these are applied in situ.

Several authors (Minafò et al., 2019; Dzaye et al., 2019; Benboudjema et al., 2013; Ruiz-Ripoll et al., 2013; Zhao et al., 2018; Mitrović et al., 2019) have already applied the DIC technique for the measurement of shrinkage in fresh concrete few minutes after mixing, validating the innovative methodology with respect to measurements performed mechanically with displacement transducers: since it is non-contact, the analysis is full-field and provides a three-dimensional (3D) view of the strains and stress. Dzaye et al. (2019) and Benboudjema et al. (Ruiz-Ripoll et al., 2013) have set-up the DIC technology for the assessment of the settlement and the shrinkage on concrete, comparing the accuracy of the measurements with the traditional ones using classical LVDT point-transducers. In particular, the DIC technique allows to measure the shrinkage already from the very first instants of mortar curing after casting inside the formwork, while the traditional mechanical measurement method with the comparator requires the hardening of the mortar, which takes place on average no earlier than 48–72 h. Ruiz-Ripoll et al. (2013) tested square concrete slabs subjected to severe conditions of restraint and moisture loss, showing the great capacity of the imaging methodology to identify and characterize the cracking pattern. Zhao et al. (2018) used the DIC technique to provide strain contour maps to understand the process of plastic shrinkage cracking inside the concrete structures. Mitrović et al. (2019) used imaging monitoring technique for analysis of shrinkage in resin-based cements and an adhesive-bonding system in daily dental practice, confirming the versatility of use of the DIC technology. Only Bertelsen et al. (2019) have deepened the study on cementitious mortars for repair reinforced concrete structures, without however extending the potential of the DIC also to the monitoring of other types of restoration mortars.

In the scientific literature there are still no measures on the diversified repair mortars used in the field of maintenance and restoration of historical buildings (included the monumental ones). In this experimental research – currently ongoing - the shrinkage of five different lime based mortars, actually used in repair works in the immediate phases following curing was measured. The test results can integrate information collected in a technical atlas on different mortar mixes for different types of maintenance works on the existing building heritage, now under developing by authors. (Grazzini et al., 2019).

## 2. Materials and methods

In these experimental tests a VIC-3D Educational system was used for measuring the shrinkage of different mortars. The system features a simplified setup, streamlined image acquisition, and ideal post-processing features (Table 1). The stereo cameras are mounted inside a protective casing, which includes an integrated LED light source and a cooling fan (Fig. 1). Previous preliminary tests were carried out by positioning the DIC on its tripod (Fig. 1a) and, subsequently, led to the creation of a fixed frame (Fig. 1b) as the optimal distance for monitoring the specimens remains constant (equal to about 50 cm) depending on the fixed characteristics of the optics of the instrumentation. The lighting of the specimens was also enhanced using LEDs and flexible lamps, placed at an optimal distance (about 50 cm) without creating light contrast on the surfaces monitored by the DIC.

The shrinkage tests were performed by packaging specimens of five mortars of different mixtures (Table 2) inside specific moulds. Since this is a first phase of the experimentation, the choice of the mixtures aimed, above all, to allow a correlation between the shrinkage phenomenon of different kinds of mortars with the evolution of the same phenomena over time and, finally, with mechanical behaviour of these mortars.

The shrinkage measurements were only performed through the DIC system in the settlement of these first exploratory tests, as the scientific literature (Tarizzo et al., 2013; Minafò et al., 2019; Dzaye et al., 2019; Benboudjema et al., 2013; Ruiz-Ripoll et al., 2013) confirmed excellent correspondence between optical and manual measurements. Total displacements pointed out by DIC can thus be compared with homologue data previously collected by manual tests. In addition, maturation

**Table 1**
Technical characteristics of VIC-3D Educational.

| Camera resolution | 1920 × 1200 (2.3 Megapixels) |
|---|---|
| **Frame Rate** | 20 Hz live, 0.5 Hz acquisition |
| **Exposure Time** | 19 μs - 1 s |
| **Field of View** | Fixed: 150 × 200 mm |
| **Displacement Resolution** | In-plane: ±2 μm; Out-of-plane: ±4 μm |
| **Strain Measurement Resolution** | 50 με |
| **Strain Measurement Range** | 0.005% to > 2000% |
| **Software Features** | 3D displacements, strains, graphing tools, etc. |

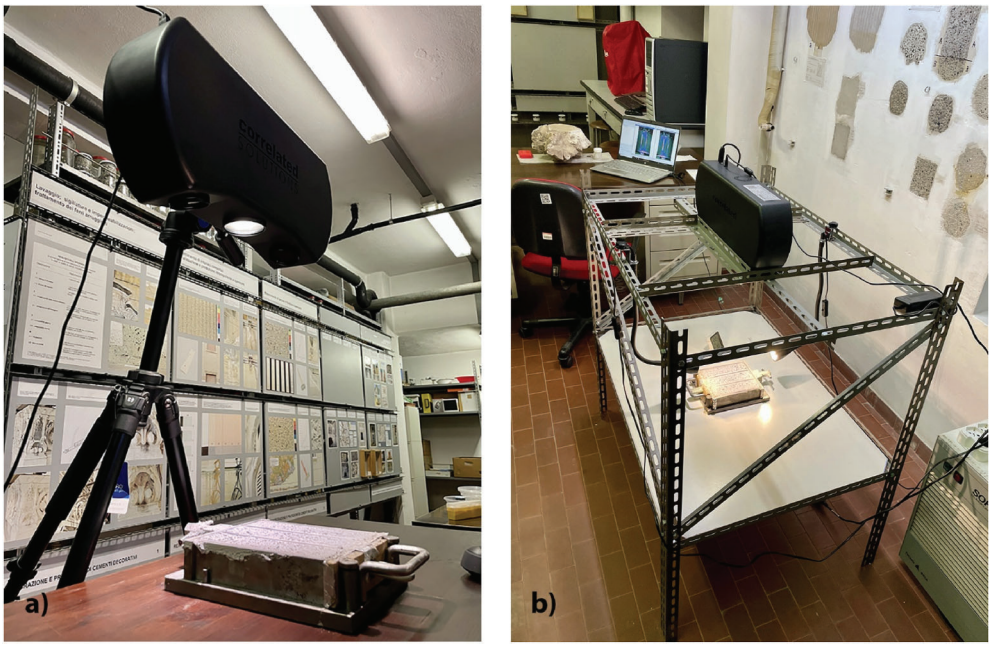


**Fig. 1.** (a) VIC-3D Educational system; (b) set-up shrinkage monitoring.

**Table 2**
Mixtures and compositions of tested mortars.

| Mix | | | | Composition* | | | | | | | |
|---|---|---|---|---|---|---|---|---|---|---|---|
| ID. | Typology | Class | Classification | Binders | | Aggregates | | Recommended Water | Water added in the sample | Binders/ Aggregates ratio** | Water/ Binders ratio** |
| | | | (EN 998-1) | [%] | | [%] | | [%] | [%] | | |
| A | Pre-dosed | Aerial | GP<br>CS II | Matured lime putty | 22–28% | Sand<br>Cocciopesto | 72–80%<br>5–12% | 4.0–12.0% | 12.00% | 0.28–0.39 | 0.14–0.55 |
| B | Pre-mixed | Hydraulic | GP<br>CS II | Natural hydraulic lime (3.5 - UNI EN 459-1, 2) | 10–20% | Sand<br>Pozzolana<br>Limestone | n/a<br>1–2.5%<br>n/a | 20.40% | 20.40% | 0.11–0.25 | 1.02–2.04 |
| C | Pre-mixed | Hydraulic | GP<br>CS II | Cement<br>Hydraulic lime | 5–10%<br>3–5% | Sand | n/a | 22.0–25.2% | 25.20% | 0.09–0.18 | 1.47–3.15 |
| D | Pre-dosed | Hydraulic | GP<br>CS IV | Cement<br>Hydraulic lime<br>Silica fumes | 8–14%<br>5–8%<br><1% | Sand | 72% | 16.00% | 16.00% | 0.15–0.30 | 0.70–1.23 |
| E | Pre-mixed | Hydraulic | GP<br>CS IV | Cement<br>Hydraulic lime | 10–20%<br>1–4% | Limestone<br>Fibers | n/a<br>n/a | 16.00% | 16.00% | 0.11–0.32 | 0.67–1.60 |

* All data are public provided by the manufacturer.
** These ratios are estimated by comparing the weights.

phases can be investigated through detailed information on the strain response of the mortar paste and the location of micro-cracks during the shrinkage time.

Optical measurement requires a pattern made up of 1 mm diameter dots, as regular as possible, applied on each specimen surface These points represent the references of the optical lens of instrumentation, to record their displacement. Originally the solution of applying the ink dots by roller was considered (Fig. 2a). However, this technique did not guarantee a uniform and complete drafting of the pattern; moreover it have to be applied on hardened surface, thus nullifying the measurement the shrinkage in the first hours after casting.

To set-up the procedure, three different types of surface pattern were settled, to evaluate the best one for the optical detection of the DIC, not interfering with phenomenon under investigation. A triad of specimens with different patterns was then tested: 0.500 mm grain size sand, black coloured a), ink applied like a spray with a little brush b) and ink on white painted surface c) (Fig. 2b). A solution of ink applied like a spray with a little brush was chosen, and a comparison of shrinkage results along the y axis pointed out an anomalous behaviour by the two other pattern types (Fig. 3). The sample with ink on a white painted surface highlighted postponed shrinkage over time, confirming evidence already known in the literature (Dzaye et al., 2019). Similarly, coloured sand seems to cause alteration after 15 h of testing. The chosen pattern also corresponds to the recommendation by the equipment manufacturer. (Fig. 4).

For each mortar, three specimens of standard size 4 × 4x16 cm (in accordance with standard UNI EN 1015-11:2007 (UNIEN 1015-11:2007, 1015)) were packaged. These moulds were chosen for many reasons. Firstly, the use of specimens with a geometry established by the standard for the mechanical characterisation tests makes it possible to subsequently subject a part of the specimens to these tests and then relate the results to those of shrinkage behaviour. It was therefore considered that

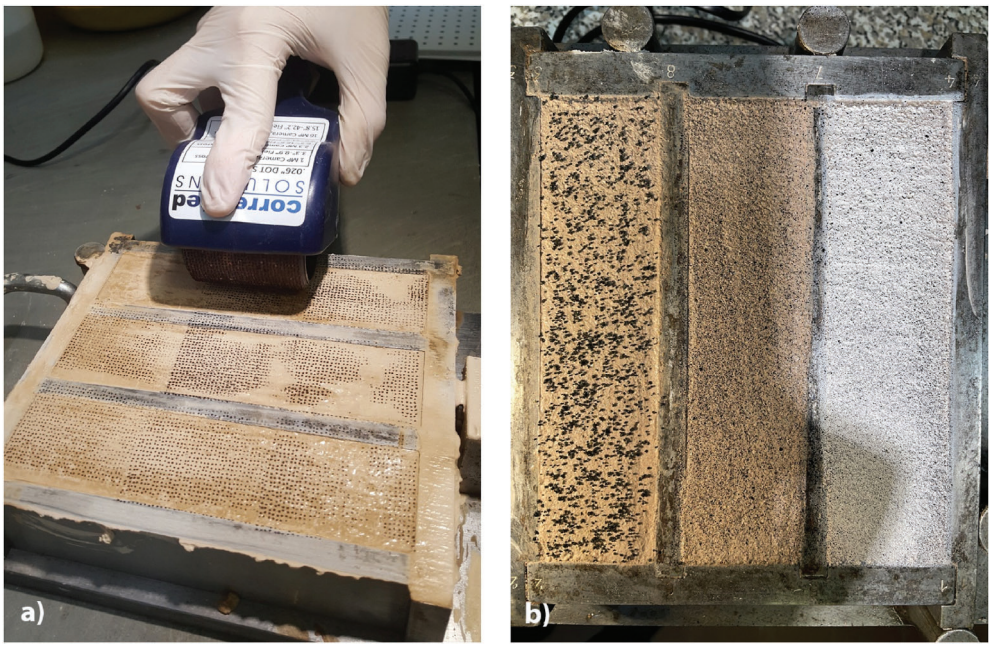


**Fig. 2.** (a) Ink roller pattern by first test; (b) Three different pattern surface by second test: 0.500 mm grain size sand, black coloured (left), ink applied with a brush (centre), ink on white painted surface (right).

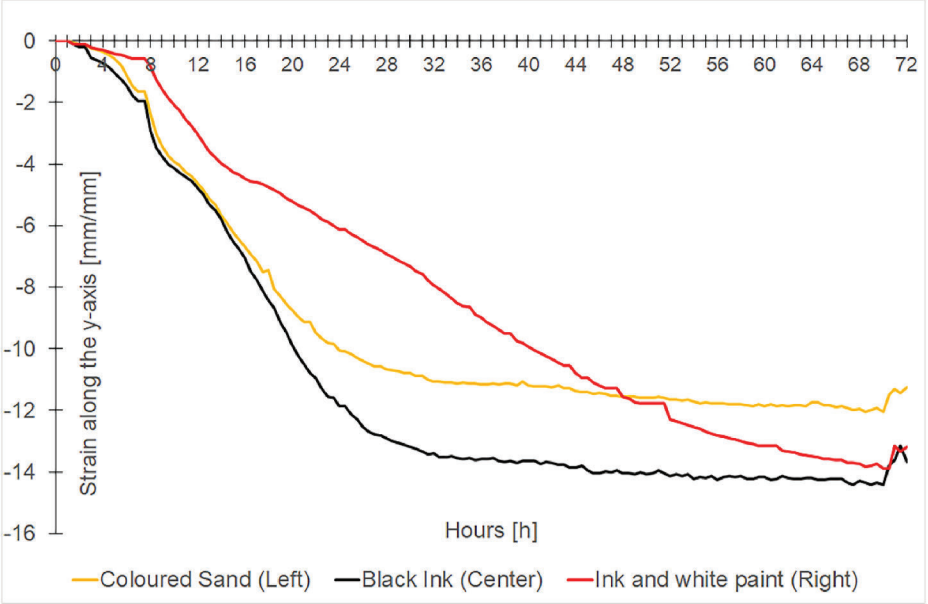


**Fig. 3.** Different shrinkage results corresponding to different patterns on the sample surfaces.

the use of these moulds could be suitable for significant observations, at the same time allowing the results obtained to be compared with mechanical performance either declared by the manufacturers (Table 3), or consolidated data in the literature. Moreover, with reference to the data known in the literature (Weiss I and Shah, 2002) about the influence of geometry on shrinkage phenomena, chosen moulds allow us to expect more significant values on the longer side (conventionally assumed as the y-axis in the test). Finally, with reference to the displacement values detectable along the z axis (depth of the test specimen, equal to 4 cm), the data obtained may already be significant with respect to the case of application in situ. As a matter of fact, the average thickness values of the plaster layers present on historical artefacts are between 3 cm and 8 cm in the majority of cases.

Once the mixing is finished, the preparatory phase begins, which includes: casting into metallic mould, consolidation on the vibration table, creating the pattern, preparing the correct lighting, setting the VIC Snap software. These operations can take 30 up to 60 min from the end of mixing, depending on the operator. For the sake of comparison, each analysis with the DIC was started after 60 min (Table 4). This time interval is essential to stabilise the accuracy of subsequent measurements, which cannot be anticipate and therefore affect the correct reading of the data collected by the DIC technique. In fact, even Dzaye et al. (2019) have detected a specific time of reliable observation (start at 130 min for cement mortars), because in the time interval preceding the irregular presence of water on the surface (bleed water) can change the consistency and position of the pattern.

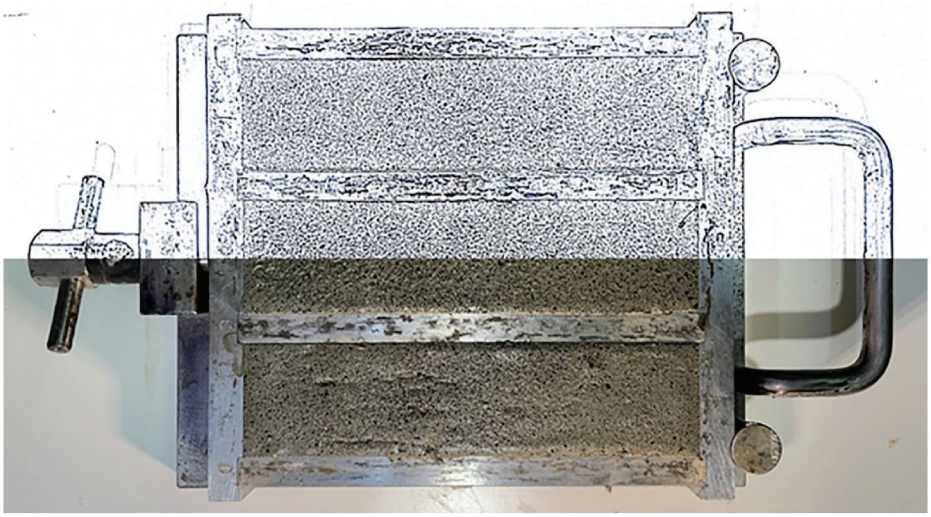

**Fig. 4.** Chosen pattern technique of the ink applied with a brush (the upper part of the image was processed by the software to better highlight the pattern).

**Table 3**
Mechanical characteristics of tested mortars.

| Mechanical performance declared by the manufacturers | | | | |
|---|---|---|---|---|
| ID. | Compressive strength after 28 days [EN 1015-11] | | Adhesion to the support [EN 1015-12] | Fracture type FP [EN 1015-12] |
| | [-] | [N/mm$^2$] | [N/mm$^2$] | [−] |
| **A** | CS II | 1,5 - 5,0 | 0,13 | A |
| **B** | CS II | 1,5 - 5,0 | 0,20 | B |
| **C** | CS II | 2,50 | ND | |
| **D** | CS IV | 8,00 | ND | |
| **E** | CS IV | 7,00 | 0,30 | A |

**Table 4**
Timing of DIC measurements.

| Timing | | | |
|---|---|---|---|
| ID. | Casting and Preparation | DIC Analysis | |
| | Start | Start | End |
| **A** | April 26, 2021 12:38 | April 26, 2021 13:38 | April 29, 2021 12:38 |
| **B** | May 17, 2021 18:00 | May 17, 2021 19:00 | May 20, 2021 18:00 |
| **C** | May 21, 2021 18:53 | May 21, 2021 19:53 | May 24, 2021 18:53 |
| **D** | May 26, 2021 17:51 | May 26, 2021 18:51 | May 29, 2021 17:51 |
| **E** | June 01, 2021 17:48 | June 01, 2021 18:48 | June 04, 2021 17:48 |
| **CHR** | June 21, 2021 18:39 | June 21, 2021 19:39 | June 24, 2021 18:39 |
| **DHR** | June 25, 2021 18:29 | June 25, 2021 19:29 | June 28, 2021 18:29 |

It was decided to carry out the analysis of all three samples present in the mould at the same time to evaluate the accuracy of the measurement and the capability of the DIC system. With respect to the DIC reference system, the x-axis lies along the short side of the specimen, the y-axis on the long side and the z-axis on the height (depth) of the specimen. Through the software it was possible to extrapolate the measurement of the shrinkage both for the single specimens and as an average of the three. All displacement analyses are with respect to a reference image acquired 1 h after the end of mixing. All analyses were performed with subsets set at 49 and a step size of 7 pixels between subset centres (Gaussian subset weights, optimized 8-tap interpolation with normalized squared differences) to obtain full-field displacement measurements. The spatial resolution is up to 12 pixels/mm. The field of view was 150 × 200 mm, with a restricted area of interest of 40 × 160 mm for each specimen.

Strains are computed in the local tangential plane of the surface, and the x-direction is taken as the projection of the global x-coordinate onto the plane; the default strain tensor used by VIC 3D was Lagrange. The shrinkage measurement test lasts 72 h, as it is believed that most of the phenomenon occurs in the first hours after casting curing, with a sampling frequency of one DIC image every 10 min. This recording frequency has been assessed sufficient for the phenomenon to be measured, in relation to previous and preliminary set-up tests of the shrinkage measurement performed with different recording frequencies. This could also be useful to subsequent definition of operative techniques for curing in situ. To understand how other internal and external factors might influence shrinkage, during the tests, humidity and temperature in the laboratory were monitored at steady intervals. Then, for two sets of mortars (C and D) the DIC analysis was repeated, placing a sensor inside the central specimen in order to measure the internal temperature and humidity (Fig. 5), thus evaluating their possible influence on shrinkage trend. The insertion of the humidity sensor inside the casting was done by connecting the sensor to one side of the formwork of the specimens.

## 3. Results

A first set of exploratory tests was useful to establish which results could be considered, with reference to the values obtained for each series of three specimens. In this specific case, it was necessary to decide whether to use the acquired values for all three samples of each set, or only for the values of the central sample, keeping the lateral samples for the subsequent mechanical characterisation tests. The comparison of the average values obtained for each specimen with the average value returned by the equipment for the three specimens made it possible to validate the reliability of the global average values (Fig. 6).

Figs. 7 and 8 show images processed on timing 72 h, with reference to the evaluation of global shrinkage strains (x-axis and y-axis, Figs. 7 and 8), and global shrinkage displacements (z-axis, Fig. 9), as the software version used does not allow the calculation of the strains along the z-axis. The graph in Fig. 10 illustrates the trend of global values as a function of the curing time of the five different materials, with reference to shrinkage strain along the y-axis, where the major retreat was expected. The negative value conventionally indicates a shortening of the specimen length, and this range was clearly the focus of the observation.

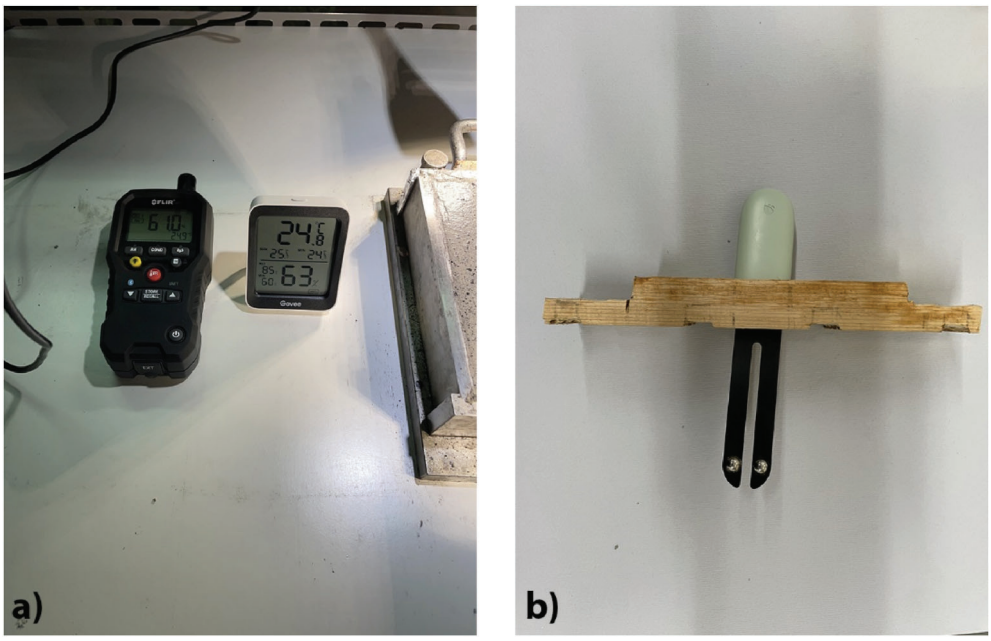


**Fig. 5.** Relative humidity measurement tools: a) external digital sensor; b) sensor inside the casting.

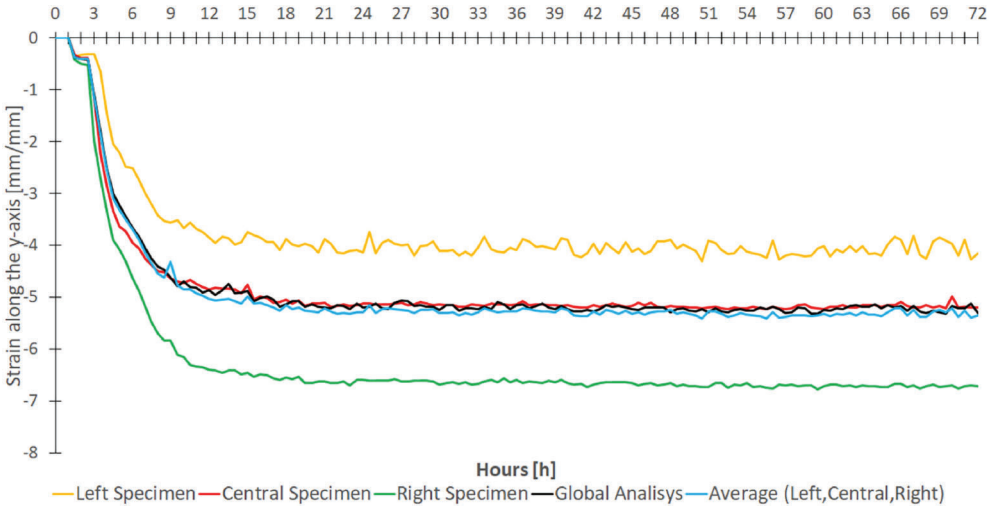


**Fig. 6.** Mortar D: graph comparing the average deformation values for each specimen in the set and the average of the values returned by the software.

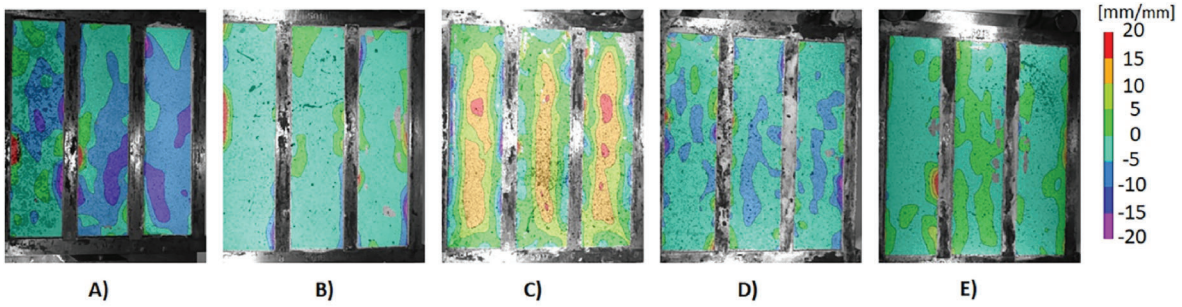


**Fig. 7.** Shrinkage strains along x axis after 72 h by DIC images corresponding to the relative types of samples (A-B-C-D-E).

These results will make it possible to acquire the characteristic average values of expected total shrinkage for each type of mortar tested. The relative graphs have been analysed, in order to determine the significant steps at which to extract the reference images, in order to conduct a detailed analysis of the mechanisms of evolution of the shrinkage phenomenon and/or relative strain stress. At the end of this

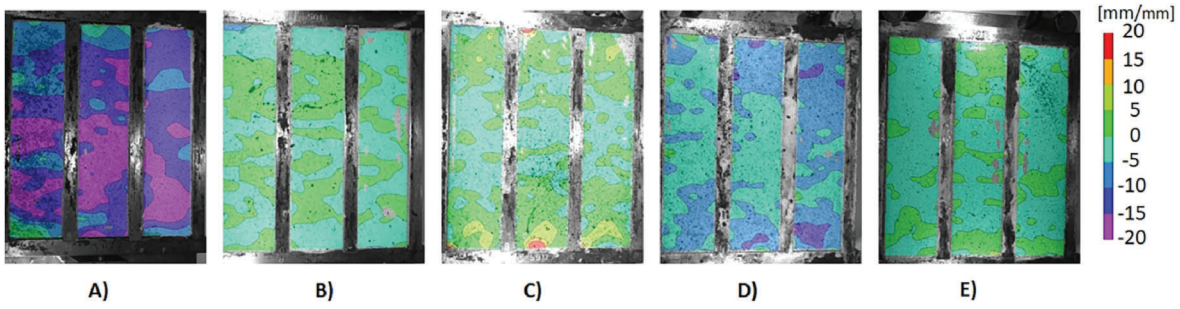


**Fig. 8.** Shrinkage strains along **y axis after 72 h by DIC images corresponding to the relative types of samples (A-B-C-D-E).**

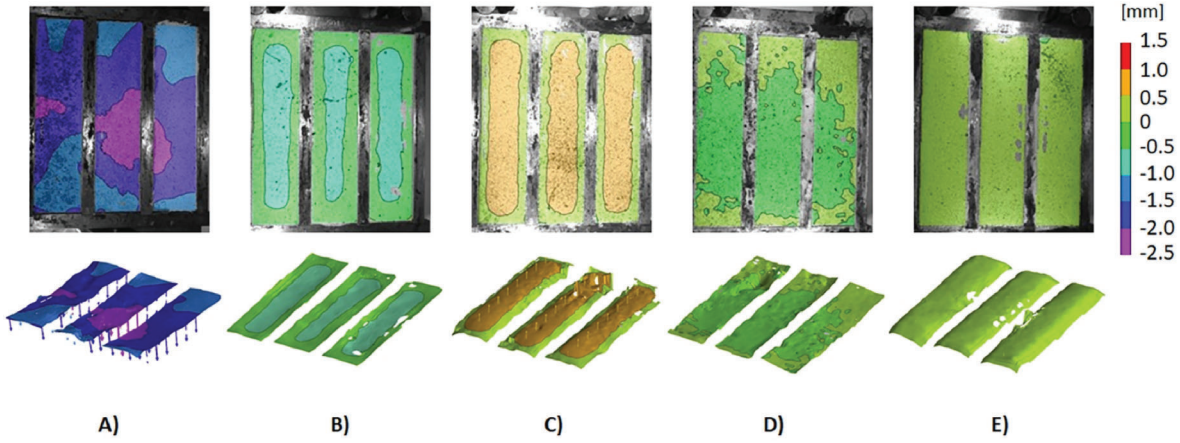


**Fig. 9.** Shrinkage displacements along z axis after 72 h by DIC images corresponding to the relative types of samples (A-B-C-D-E).

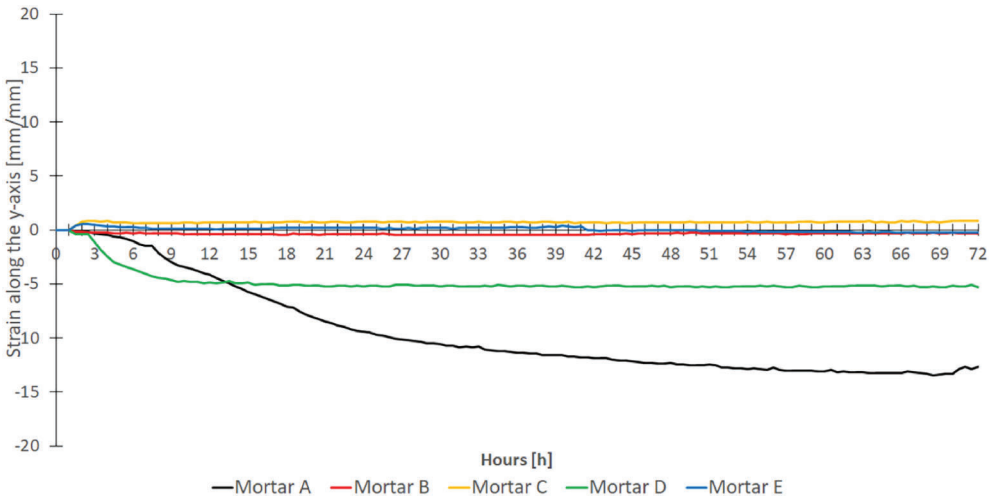


**Fig. 10.** Shrinkage strain along y axis (average values calculated by the software).

first set of tests, it was decided to take 3 h, 6 h, 9 h, 12 h, 24 h, 36 h and 72 h as snapshots for comparison. Figs. 11–13 show the graphs for strain along the y-axis, with reference to three of the five mortars considered.

On the basis of the results obtained and illustrated above, two mortars were identified with which to repeat the tests by applying a sensor inside the test specimen to monitor the RH and temperature conditions inside the test specimen. This was done in order to highlight any correlations with the shrinkage phenomenon during the first three days of curing. Mortar A has been excluded, since mortars with coccopesto will be tested later on.

It has therefore been decided to dedicate this more in-depth study to the two mortars whose first sets of tests highlighted the greatest deformation phenomena, in absolute value. The graphs in Figs. 14 and 15 illustrate the respective curves, showing the monitoring results, in order to highlight the influence of the environmental conditions on the progressive water bleeding phenomenon and its subsequent evaporation from the specimens.

Finally, the RH values were compared with the shrinkage trend in order to detect its influence on the phenomenon under observation. The graphs in Fig. 16 illustrate the correlation of the deformation values

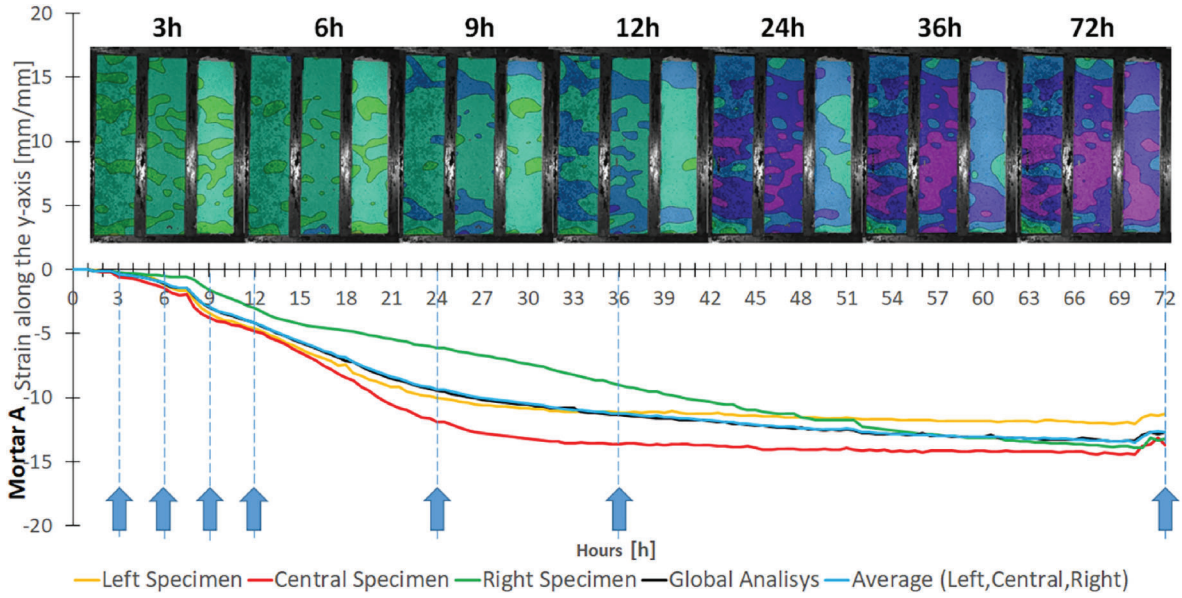


**Fig. 11.** Mortar A: average shrinkage strain along y axis at each defined step of observation.

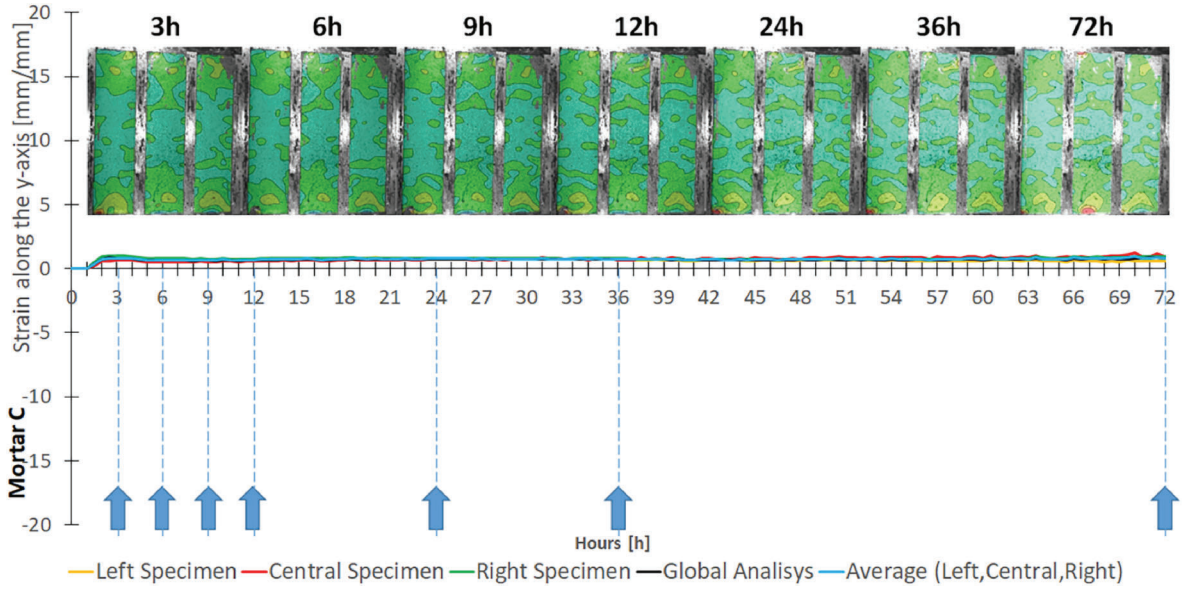


**Fig. 12.** Mortar C: average shrinkage strain along y axis at each defined step of observation.

along the y axis for mortars C and D, respectively.

## 4. Discussion

In general, during tests it was found that larger length variations were measured along the y-axis corresponding to longer side of specimens. Results showed that shrinkage occurs with maximum values especially in the first hours of the maturation, and then diminishes over time. As can be seen from the graphs after a certain time interval (which varies according to the type of mortar), the shrinkage phenomenon, recorded as a global average value, tends to stabilise. However, the comparative reading of the graphs and the images acquired, shows an evolution of the deformation states, which in some cases are concentrated in specific areas of the samples. This supports the hypothesis of an interest in the development of further sets of tests, to be applied to materials with similar compositions, operating variations of single variables at each step of investigation (influence of the binder water ratio, of the aggregate binder ratio, of the size of the aggregates, of the size and concentration of the reinforcement fibres, e.g).

With reference to the nature and characteristics of the five varieties of mortar discussed in this study, several observations may already be made, which can aid in understanding any unique aspects of the shrinkage phenomenon. As mentioned above, the five repair mortars tested have different characteristics in terms of components and mechanical performances (Table 3): shrinkage was more pronounced only on the pre-dosed mortars (A and D) as also visible in Figs. 7 and 8, while for the others it was of modest size.

In particular, mortar A, contains *cocciopesto*: as well known, *cocciopesto* has a strong ability to absorb water in the mortar curing stage, if the brick granules are not in "wet with dry surface" condition. In fact, mortar A recorded the greatest shrinkage, ever increasing during the 72 h of monitoring. To reduce the phenomenon in *cocciopesto* mortars, possible way is to add to the mixture granules saturated with water but with the surface dry.

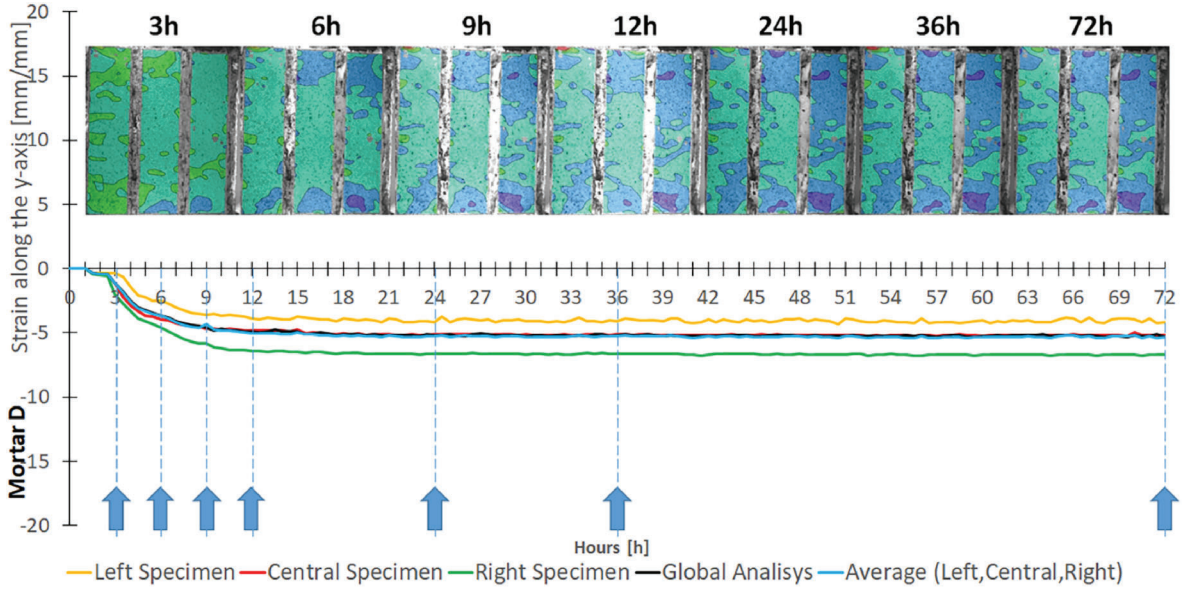


**Fig. 13.** Mortar D: average shrinkage strain along y axis at each defined step of observation.

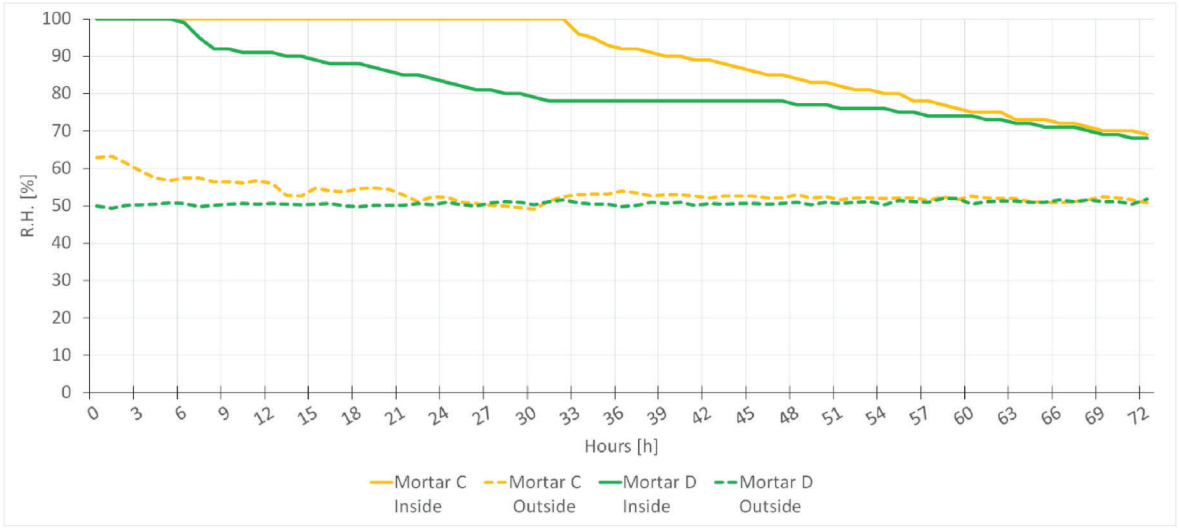


**Fig. 14.** Graph showing R.H. monitored in the environment and internal trends in the samples of mortars C and D (second set of tests).

Analysis of shrinkage global values (strain and displacement) for mortar D shows a significant increase in shrinkage from the beginning up to about 9–12 h, then tending to stabilise.

The comparison of the detailed mapping of the surfaces, however, allows further differences to be noted. Mortar A in fact shows the greatest values of negative deformation in the centre of the sample, while the opposite condition is recorded for mortar D and (although with less significant differences in numerical terms) for mortars C and D. This suggests a possible different behaviour of the materials with regard to edge adhesion, e.g. in the case of patching existing surfaces.

Mortars B and E are the two others with apparently similar behaviour with regard to the global shrinkage values, recorded 72 h after casting (see Figs. 7 and 8). In terms of phenomenon evolution, mortar B showed consistent minimal shrinkage throughout the test. Mortar E began to shrink after about half of the test, with very little deformation. On the other hand, from the mapping, it is evident that the distribution of the shrinkage and deformation values highlighted on the surface of mortar type E, unlike that of mortar type B, is substantially uniform. This is consistent with the expected characteristics of a mortar with fibre additives, like mortar E.

The only mortar that did not retreat was mortar C: it is possible that the premixed mortar, as is often the case – but is not declared in the technical data sheets – is additivated with CE – cellulose ether modified – to obtain a good water retention and, consequently, a shrinkage practically zero. Fig. 7 confirms a slight swelling in contrast to other mortars.

These observations appear to be of interest from the perspective of setting up guidelines for the operative methods of application of materials on site, specific for the different types of materials, which in part are known, but which thanks to the application of the test method currently being defined can be usefully correlated to the characteristics of the constitution, instead of aseptically deduced from a technical data sheet. This is the case, for example, with the control/monitoring of RH and internal T, which will be discussed below.

In this regard, it should be noted that the results obtained refer to behaviour in environmental conditions that could be defined as sub-controlled, i.e. different from the conditions to which the materials applied in situ are subjected (daily temperature range, and relative

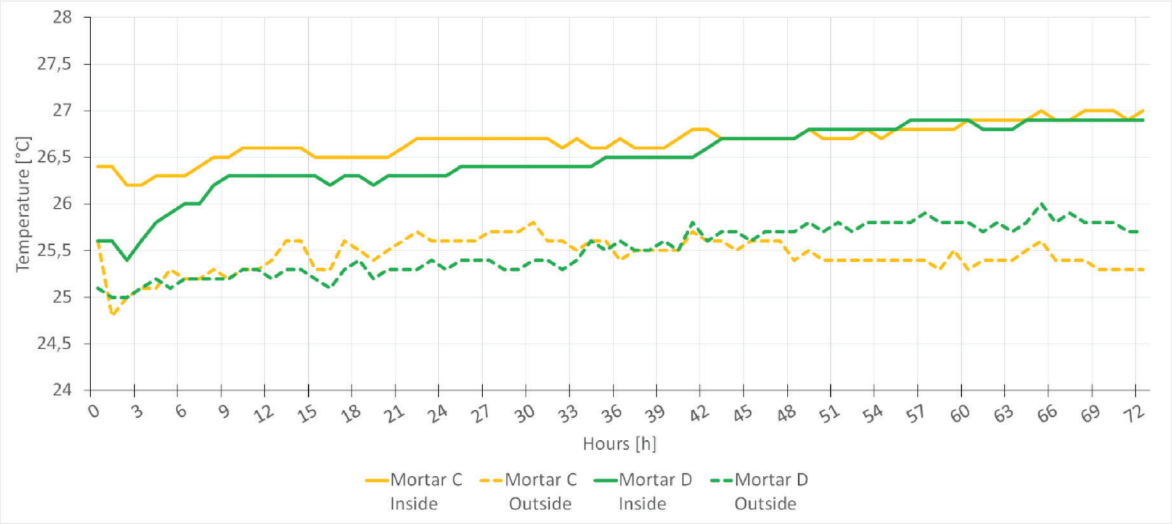


**Fig. 15.** Graph showing Temperature monitored in the environment and internal trends in the samples of mortars C and D (second set of tests).

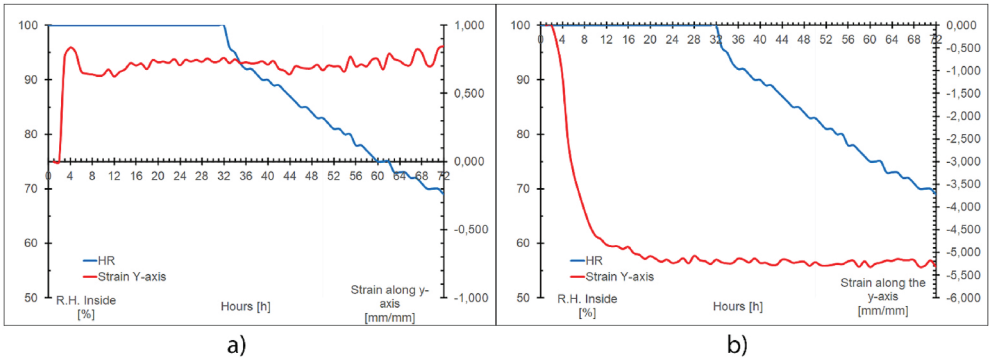


**Fig. 16.** Variation of strains in relation to humidity measured within the specimens for mortar C (a) and mortar D (b).

humidity conditions, for example). Operating under laboratory conditions is also necessary in order to have a reliable basis for comparison of the data obtained. At the same time, it is necessary to be able to estimate the sensitivity of the phenomena observed with respect to the parameters of humidity and temperature. For this reason, two of the most representative samples of the different shrinkage behaviours were selected for internal moisture control.

The graphs in Figs. 14 and 15 show the variations in relative humidity and internal and external temperatures recorded for the type C and D mortar specimens. It was interesting to observe the relationship between the shrinkage trend and the change in the amount of internal moisture in the two samples compared. The external humidity of the specimen has always remained almost constant, while the internal humidity has undergone a decrease of up to about 70%. This is due to the internal curing processes of the casting (Fig. 16).

With regard to the influence of two important variables, the binder water ratio and the aggregate binder ratio, and their influence on the shrinkage phenomenon (Yang et al., 2017; Zhang et al., 2014), these first tests have not been carried out to evaluate them, nor do they allow a comparative analysis to be made. In fact, as highlighted in Table 2, the five mortars used have been chosen among the most widely used mortars on the market, without modifying their formulation and using a quantity of mixing water consistent with the manufacturer's indications, which is adequate in all cases, both in terms of workability and in terms of the shrinkage values obtained.

## 5. Conclusions and perspectives

Shrinkage, together with resulting micro-cracks, represent one of the main problems affecting repair mortars, especially those for the recovery of ancient historical plasters, as they are often the cause of premature deterioration and loss of effectiveness of the restoration works. The presence of cracks also compromises the aesthetic aspect. Hygrometric shrinkage of repair mortars can also affect the adhesion to the existing substrate as sometimes can be found in the underlying layer of existing plaster at the contact surface, causing early detachments (Grazzini et al., 2020). As these problems are common to all types of mortars that could be used for architectural recovery, results of this research aim to be useful to compare shrinkage tendency of different repair mortars and to enable the choices and applications of those more compatible case by case with heritage involved in maintenance and restoring interventions.

The first phase of this experimentation had been addressed to calibrate the optical survey of the DIC by investigating the shrinkage of five repair mortars with very different performances (in the first phase of this research, only commercial products were used). This optical technique, has shown excellent potential in the measurement accuracy and deepen of a complex phenomenon such as that of the shrinkage of mortars. For these reasons, in the following steps this research will investigate the extent of the shrinkage of different types of repair mortars to assess their durability against the different substrates on which they can be applied. In this sense, one focus is to integrate an under-construction atlas about the behaviour of different mortar mixes (Lindqvist, 2009) also with the information regarding the hygrometric shrinkage, which many

producers omit on the technical data sheets of the currently marketed repair mortars (relevant information when data and results are available as a result of a specific and correct diagnostic campaign). Moreover, testing many kinds of mortar mixes keeping the aggregate size distribution constant, has the target of introducing only one variable at a time (e.g., aggregate/binder ratio).

The innovation in method proposed by the on-going research, is to exploit the potential of DIC technique in order to deepen and characterize differences in the behaviour of a significant number of materials that are mistakenly considered similar in practice. The achieved results, in fact, highlights differences in the measures of shrinkage between different mixing mortars, and therefore highlight the importance of choices to guarantees satisfactory durability in relation to the context in which it will be applied. 2D strains visualization maps help interpret shrinkage in the first hours of mortar curing. The DIC technique allows measurement of non-uniform surface displacement due to material heterogeneity and geometry affecting shrinkage distribution that cannot be detected by traditional transducers.

The experimental research will continue with further refinements of the methodology and will compare the optical measurements with the manual ones using a mechanical comparator. Furthermore, the range of choice of mortars will be extended, also favouring those with handcrafted packaging over premixed ones. In this way, experimental research will also become an opportunity to validate the use of traditional mortar mixes to be re-proposed in restoration sites, not only prepared by graduated Restorers (for monuments, e.g.) but also by craftsmen that – currently – have loss the capability to prepare appropriate mortar and concrete mixes *in opera*.

The results will be collected in the set-up of an-going atlas of references, compared to many mixtures of mortars and conglomerates, intended as on operative and dynamic tools to support the operational choices in the project of restoration, recovery, and maintenance of historical buildings (Grazzini et al., 2019).

## Declaration of competing interest

The authors declare that they have no known competing financial interests or personal relationships that could have appeared to influence the work reported in this paper.

## Acknowledgements

The authors wish to thank the MAIN10ANCE Interreg ITA-CH Project (European Community, ID 473472) for funding the DIC device used for the measurements in this experimental research.

## References

Benboudjema, F., Mauroux, T., Turcry, P., Ait-Mokthar, A., 2013. Experimental analysis of drying shrinkage cracking in coating mortars by digital image correlation. In: Proc. of the 9th Int. Conf. on Creep, Shrinkage, and Durability Mechanics, CONCREEP, vols. 235–242. American Society of Civil Engineers, Cambridge MA, United States, p. 100719. https://doi.org/10.1061/9780784413111.027, 22-25 September 2013, (ASCE).

Bertelsen, I.M.G., Kragh, C., Cardinaud, G., Ottosen, L.M., Fischer, G., 2019. Quantification of plastic shrinkage cracking in mortars using digital image correlation. Cement Concr. Res. 123, 105761 https://doi.org/10.1016/j.cemconres.2019.05.006.

Bocca, P., Grazzini, A., 2013. Mechanical properties and freeze-thaw durability of strengthening mortars. J. Mater. Civ. Eng. 25, 274–280. https://doi.org/10.1061/(ASCE)MT.1943-5533.0000597.

Bocca, P., Grazzini, A., Masera, D., Alberto, A., Valente, S., 2011. Mechanical interaction between historical brick and repair mortar: experimental and numerical tests. J. Phys. (Paris): Conf. Series. 305, 012126 https://doi.org/10.1088/1742-6596/305/1/012126.

RILEM TC 167-COM, 2005. Characterization of Old Mortars with Respect to their Repair. Introduction to requirements for and functions and properties of repair mortars. Mater. Struct. 38, 781–785. https://doi.org/10.1617/14319.

Dzaye, E.D., Tsangouri, E., Spiessens, K., De Schutter, G., Aggelis, D.G., 2019. Digital image correlation (DIC) on fresh cement mortar to quantify settlement and shrinkage. Arch. Civil Mech. Eng. 19, 205–214. https://doi.org/10.1016/j.acme.2018.10.003.

Grazzini, A., Zerbinatti, M., Fasana, S., 2019. Mechanical characterization of mortars used in the restoration of historical buildings: an operative atlas for maintenance and conservation. IOP Conf. Ser. Mater. Sci. Eng. 629, 012024 https://doi.org/10.1088/1757-899X/629/1/012024.

Grazzini, A., Lacidogna, G., Valente, S., Accornero, F., 2020. Acoustic emission and numerical analysis of the delamination process in repair plasters applied to historical walls. Construct. Build. Mater. 236, 117798 https://doi.org/10.1016/j.conbuildmat.2019.117798.

Lindqvist, J.E., 2009. Rilem TC 203-RHM: repair mortars for historic masonry. Testing of hardened mortars, a process of questioning and interpreting. Mater. Struct. 42, 853–865. https://doi.org/10.1617/s11527-008-9455-x.

Minafò, G., La Mendola, L., D'Anna, J., Amato, G., Chen, J.F., 2019. On the use of digital image correlation (DIC) for evaluating the tensile behaviour of BFRCM strips. Key Eng. Mater. 817, 377–384. https://doi.org/10.4028/www.scientific.net/KEM.817.377.

Mitrović, A., Antonović, D., Tanasić, I., Mitrović, N., Bakić, G., Popović, D., Milošević, M., 2019. 3D Digital Image Correlation Analysis of the Shrinkage Strain in Four Dual Cure Composite Cements. BioMed Res. Int., 2041348 https://doi.org/10.1155/2019/2041348. ID.

Ruiz-Ripoll, L., Barragán, B.E., Moro, S., Turmo, J., 2013. Digital imaging methodology for measuring early shrinkage cracking in concrete. Strain 49, 267–275. https://doi.org/10.1111/str.12034.

Tarizzo, P., Formia, A., Tulliani, J.M., Zerbinatti, M., Schiavi, A., 2013. A new non-invasive method to evaluate the detachments of plasters. First results. Int. J. Conserv. Sci. 4, 587–592.

UNI EN 1015-11:2007, Methods of Test for Mortar for Masonry - Part 11: Determination of Flexural and Compressive Strength of Hardened Mortar .

Weiss I, W.J., Shah, S.P., 2002. Restrained shrinkage cracking: the role of shrinkage reducing admixtures and specimen geometry. Mater. Struct. 35, 85–91. https://doi.org/10.1007/BF02482106.

Yang, J., Wang, Q., Zhou, Y., 2017. Influence of curing time on the drying shrinkage of concretes with different binders and water-to-binder ratios. Adv. Mater. Sci. Eng., 2695435 https://doi.org/10.1155/2017/2695435, 2017, Article ID.

Zhang, J., Dong Han, Y., Gao, Y., 2014. Effects of water-binder ratio and coarse Aggregate,Content on interior humidity, autogenous shrinkage, and drying shrinkage of concrete. J. Mater. Civ. Eng. 26 https://doi.org/10.1061/(ASCE)MT.1943-5533.0000799.

Zhao, P., Zsaki, A.M., Nokken, M.R., 2018. Using digital image correlation to evaluate plastic shrinkage cracking in cement-based materials. Construct. Build. Mater. 182, 108–117. https://doi.org/10.1016/j.conbuildmat.2018.05.239.